Constrained matched filtering for extended dynamic range and improved noise rejection for Shack–Hartmann wavefront sensing

L. Gilles* and B. L. Ellerbroek

Thirty Meter Telescope Observatory Corporation, 1200 East California Boulevard, Mail Code 102-8, Pasadena, California 91125, USA

**Corresponding author: lgilles@caltech.edu*

Received February 5, 2008; revised April 2, 2008; accepted April 3, 2008; posted April 17, 2008 (Doc. ID 92515); published May 14, 2008

We recently introduced matched filtering in the context of astronomical Shack–Hartmann wavefront sensing with elongated sodium laser beacons [Appl. Opt. **45**, 6568 (2006)]. Detailed wave optics Monte Carlo simulations implementing this technique for the Thirty Meter Telescope dual conjugate adaptive optics system have, however, revealed frequent bursts of degraded closed loop residual wavefront error [Proc. SPIE **6272**, 627236 (2006)]. The origin of this problem is shown to be related to laser guide star jitter on the sky that kicks the filter out of its linear dynamic range, which leads to bursts of nonlinearities that are reconstructed into higher-order wavefront aberrations, particularly coma and trifoil for radially elongated subaperture spots. An elegant reformulation of the algorithm is proposed to extend its dynamic range using a set of linear constraints while preserving its improved noise rejection and Monte Carlo performance results are reported that confirm the benefits of the method. © 2008 Optical Society of America

OCIS codes: 010.1080, 010.7350.

In the framework of Shack–Hartmann wavefront sensing, matched filtering refers to noise-weighted least-squares estimation of subaperture spot displacements from detector pixel intensities. The filter is based upon the following linearized subaperture pixel intensity vector model versus input subaperture wavefront tilt [1]:

$$I_\star(\theta) = I_0 + G\theta + \eta, \tag{1}$$

where $I_\star$ denotes the model detector pixel intensity vector, θ is the input subaperture wavefront tilt variable, I_0 is the model noise-free detector pixel intensity vector at null, $G=\partial I_\star/\partial\theta$ is the model pixel intensity gain (Jacobian) matrix, and η is the model measurement noise vector of zero ensemble mean and covariance matrix $C_\eta=\mathrm{diag}(I_0+\sigma^2)$, where σ is the detector read noise. Pixel intensities are assumed to be given in units of photodetected events (pde), and θ in units of the detector pixel angular subtense. Note that the model described in Eq. (1) requires knowledge of (i) the reference intensity vector I_0 and (ii) the gain matrix G. These two quantities depend upon the laser beam profile, the atmospheric seeing, and the internal structure of the mesospheric sodium layer [1]. In practical implementations they are computed via temporal low-pass filtering and dithering background processes that update them in real time at an appropriate bandwidth [2]. For the purpose of this study, the isoplanatic short-exposure model reported in [1] has been adopted under the assumption of a perfect *a priori* knowledge of the above physical quantities. The particular form of the imaging model used to compute I_0 and G is not critical to the analysis.

Matched filtering minimizes pixel intensity discrepancy, which is the average difference between the actually measured pixel intensity vector I and $I_\star$:

$$\hat{\theta} = \arg\min_\theta \langle \|I - I_\star(\theta)\|^2 \rangle = R(I - I_0), \tag{2}$$

where $\langle\,\rangle$ denotes ensemble average and R is the noise-weighted left-inverse of the gain matrix G, i.e.,

$$R = (G^T C_\eta^{-1} G)^{-1} G^T C_\eta^{-1}. \tag{3}$$

The model noise equivalent angle covariance matrix associated with the linear filter R is given by the following expression:

$$C_\theta = R C_\eta R^T = (G^T C_\eta^{-1} G)^{-1}. \tag{4}$$

To avoid estimation bias induced by signal level variations, it is desirable to modify the matched filter to null RI_0, in which case the estimate would be given by

$$\hat{\theta} = RI. \tag{5}$$

Straightforward Lagrange multiplier manipulations show that such a filter can be found and is given by the following equation:

$$R = M(G_e^T C_\eta^{-1} G_e)^{-1} G_e^T C_\eta^{-1}, \tag{6}$$

$$M = \begin{bmatrix} 1 & 0 & 0 \\ 0 & 1 & 0 \end{bmatrix}, \quad G_e = \begin{bmatrix} G & I_0 \end{bmatrix}, \tag{7}$$

where M and G_e denote, respectively, the matrix containing the constraints and the extended gain matrix. Note that $RG_e=M$; that is, (i) the filter has the correct gain at the origin (i.e., it correctly estimates small displacements for which pixel intensities are linear in the subaperture tilt), and (ii) RI_0 is nulled.

Using our in-house developed Linear Adaptive Optics Simulator (LAOS) software, detailed wave optics Monte Carlo simulations implementing such a filter

0146-9592/08/101159-3/$15.00 © 2008 Optical Society of America

for the Thirty Meter Telescope (TMT) dual conjugate adaptive optics (AO) system have, however, revealed frequent bursts of degraded closed loop residual wavefront error [3]. An elegant solution to this problem is proposed here through four additional linear constraints that force the filter to correctly estimate displacements of ±1 pixel in both measurement directions from ideal noise-free images, thereby increasing its linear dynamic range. The resulting constrained filter has the same form as in Eq. (6), but with M and G_e replaced by the following extended expressions:

$$M = \begin{bmatrix} 1 & 0 & 0 & 1 & -1 & 0 & 0 \\ 0 & 1 & 0 & 0 & 0 & 1 & -1 \end{bmatrix},$$

$$G_e = \begin{bmatrix} G & I_0 & I_1 & I_2 & I_3 & I_4 \end{bmatrix}, \quad (8)$$

where I_1 and I_2 denote intensity vectors obtained from a ±1 pixel shift along the rows of the array representation of I_0, and similarly I_3 and I_4 are for shifts along the columns of that array. Since no information is available outside the array, zeros are assigned to the appropriate boundary pixels. Note that since $RG_e = M$, there is no estimation error for displacements of ±1 pixel. Note also that the constrained filter R does not increase real time computation requirements since its size is preserved.

Simulation results reported below are for a 30 m circular aperture, a 1/2 m centrally located laser projecting aperture, an order of 60×60 Shack–Hartmann wavefront sensor imaging an on-axis sodium laser guide star (LGS) at 90 km range, and an order of 60×60 piezodeformable mirror conjugate to ground level with actuators at subaperture vertices (Fried geometry). Only a single ground-layer translating von Karman turbulence phase screen has been simulated to eliminate the cone effect and allow meaningful comparisons of different algorithms without the additional complexity of modeling atmospheric tomography and multiconjugate adaptive optics. The outer scale was chosen equal to 30 m, the wind speed equal to $v = 10$ m/s, and at 500 nm the Fried parameter was $r_0 = 15$ cm and the Greenwood frequency was approximately $(0.102/0.42)^{3/5} v/r_0 = 29$ Hz. A sparse approximation of the open loop minimum variance wavefront reconstructor obtained by adjusting the regularization term has been used in conjunction with a deformable mirror (DM) observer, a technique refered to as "pseudo-open-loop control" [4]. The AO loop frame rate is 800 Hz with a 30 Hz closed loop bandwidth and a 30 Hz laser pointing loop bandwidth. The uncompensated (turbulence induced) laser tip–tilt jitter on the sky is of the order of 285 mas. A signal level of 900 pde per subaperture per integration time has been assumed, which is the expected median return flux from a 25 W cw sodium laser and is the requirement imposed upon the TMT LGS facility. Finally, a polar coordinate CCD array [5] with $16 \times 4\,500$ mas pixels per subaperture aligned along the elongation direction and 3 electrons readout noise per pixel has been assumed.

Figure 1 illustrates sample performance results on noise-free data for a scenario with an elongated laser beacon and the polar coordinate CCD array with $16 \times 4\,500$ mas pixels per subaperture. By noise free we mean that the detector pixel intensities did not include addtitive Poisson and Gaussian noise contributions. The dots on the LGS trajectories correspond to the three first bursts of degraded closed loop residual wavefront error. Note that these occur at excursions of the LGS trajectory on the sky exceeding 100 mas. The constrained filter clearly features lower nonlin-

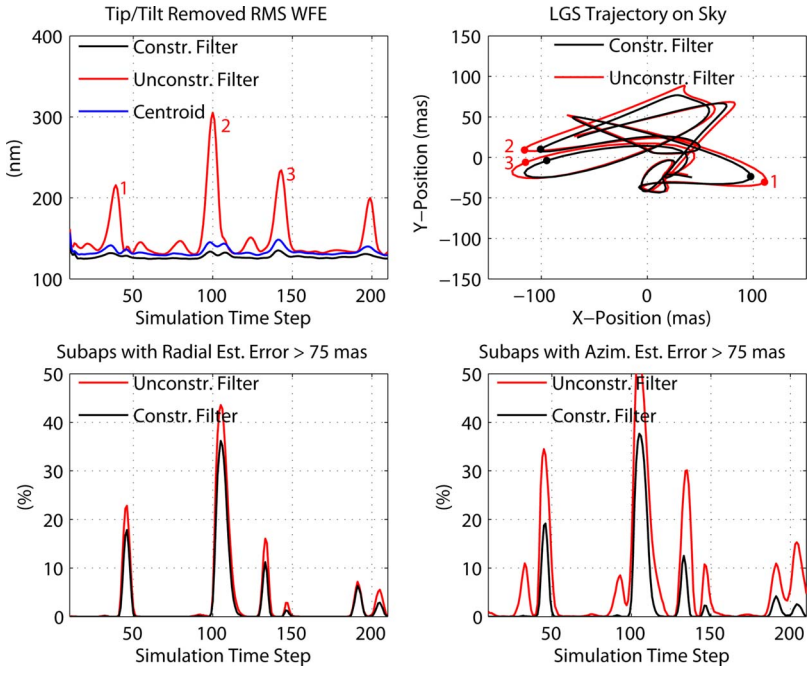

Fig. 1. (Color online) Sample performance results on noise-free data for a scenario with an elongated beacon and the polar coordinate CCD array with $16 \times 4\,500$ mas pixels per subaperture. The dots on the LGS trajectories correspond to the three first bursts of degraded closed loop residual wavefront error.

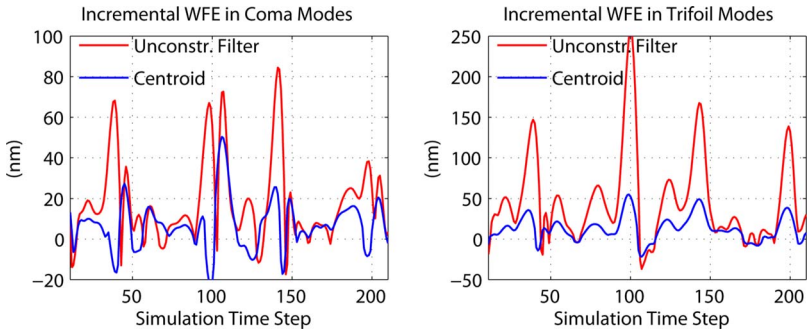

Fig. 2. (Color online) Upper panels display the incremental wavefront error (in quadrature) in the coma and trifoil Zernike modes from the constrained filter results shown in Fig. 1.

earities and the lowest closed loop residual wavefront error.

Figure 2 illustrates that, for radially elongated spots, bursts of nonlinearities are predominantly reconstructed into coma and trifoil aberrations.

Finally, Fig. 3 displays the wavefront error (in quadrature) owing to measurement noise for the atmospheric phase screen used in Fig. 1 and for a signal level of 900 pde per subaperture per integration time and 3 electrons readout noise per pixel. Remarkably, the constraints do not degrade the excellent noise rejection properties of the filter, and superior performance is obtained compared to what is achievable with a conventional centroiding algorithm.

In conclusion, we have shown in this Letter that the original matched filter developed by the authors for improved noise rejection for Shack–Hartmann wavefront sensing suffers from limited linear dynamic range. A reformulation of the model forcing the filter to correctly estimate displacements of ±1 pixel in both measurement directions provides an adequate linear dynamic range while still preserving superior noise rejection compared to a conventional centroiding algorithm. Finally, note that the benefits of the constrained filter described in this Letter apply equally to laser and natural guide star (NGS) Shack–Hartmann wavefront sensing.

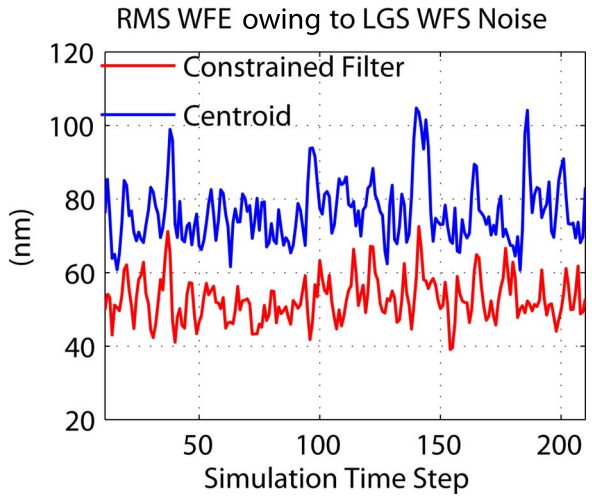

Fig. 3. (Color online) Wavefront error owing to measurement noise for the same atmospheric phase screen used in Fig. 1 and for a signal level of 900 pde per subaperture per integration time and 3 electrons readout noise per pixel.

The authors gratefully acknowledge the support of the TMT partner institutions. They are the Association of Canadian Universities for Research in Astronomy (ACURA), the California Institute of Technology, and the University of California. This work was supported as well by the Gordon and Betty Moore Foundation, the Canada Foundation for Innovation, the Ontario Ministry of Research and Innovation, the National Research Council of Canada, the Natural Sciences and Engineering Research Council of Canada, the British Columbia Knowledge Development Fund, the Association of Universities for Research in Astronomy (AURA), and the U.S. National Science Foundation.

References

1. L. Gilles and B. L. Ellerbroek, Appl. Opt. **45**, 6568 (2006).
2. G. Herriot, R. Conan, O. Lardière, D. Andersen, B. Ellerbroek, L. Gilles, P. Hickson, K. Jackson, J. P. Véran, and L. Wang, "Compensation of TMT laser wavefront sensors for variations of sodium layer," Proc. SPIE (to be published).
3. L. Gilles, B. L. Ellerbroek, and J. P. Véran, Proc. SPIE **6272**, 627236 (2006).
4. L. Gilles, Appl. Opt. **44**, 993 (2005).
5. S. M. Adkins, O. Azucena, and J. E. Nelson, Proc. SPIE **6272**, 62721E (2006).